

The $s = \frac{1}{2}$ Antiferromagnetic Heisenberg Model on Fullerene-Type Symmetry Clusters

N. P. Konstantinidis*

*Department of Physics and Department of Mathematics,
University of Dublin, Trinity College, Dublin 2, Ireland*

(Dated: May 6, 2019)

The $s_i = \frac{1}{2}$ nearest neighbor antiferromagnetic Heisenberg model is considered for spins sitting on the vertices of clusters with the connectivity of fullerene molecules and a number of sites n ranging from 24 to 32. Using the permutational and spin inversion symmetries of the Hamiltonian the low energy spectrum is calculated for all the irreducible representations of the symmetry group of each cluster. Frustration and connectivity result in non-trivial low energy properties, with the lowest excited states being singlets except for $n = 28$. Same hexagon and same pentagon correlations are the most effective in the minimization of the energy, with the $n = 32 - D_{3h}$ symmetry cluster having an unusually strong singlet intra-pentagon correlation. The magnetization in a field shows no discontinuities unlike the icosahedral I_h fullerene clusters, but only plateaux with the most pronounced for $n = 28$. The spatial symmetry as well as the connectivity of the clusters appear to be important for the determination of their magnetic properties.

PACS numbers: 75.10.Jm Quantized Spin Models, 75.50.Ee Antiferromagnetics, 75.50.Xx Molecular Magnets

I. INTRODUCTION

The antiferromagnetic Heisenberg model (AHM) has been the object of intense investigation for some time now as a prototype of strongly correlated electronic behavior. The effects of frustration, quantum fluctuations and low dimensionality can lead to new phases differing from conventional order and possessing a non-trivial low energy spectrum [1, 2, 3]. Small magnetic clusters provide an excellent testing ground for the validity of the AHM as well as other theoretical models, as oftentimes its low energy properties can be computed on these structures and its predictions can be directly tested against experiments [4].

The fullerenes are a class of three-fold coordinated molecules consisting of $\frac{n}{2} - 10$ hexagons and 12 pentagons, with n their number of vertices (or sites) [5]. With increasing n their shape resembles more and more the honeycomb lattice, albeit in closed form, with the pentagons playing the role of structural impurities. Frustration decreases with n , as the unfrustrated hexagons dominate in number the frustrated pentagons, while the distribution of the latter determines the symmetry group of the molecule. The properties of the AHM have been computed for the smallest element of the family, the dodecahedron, which consists only of pentagons and belongs to the icosahedral point symmetry group I_h . For classical spins the signature of frustration is very strong, generating three magnetization discontinuities in an external magnetic field, unexpectedly for a model lacking magnetic anisotropy [6, 7]. In the full quantum limit where the individual spin magnitude $s_i = \frac{1}{2}$, the low energy spectrum consists of singlets, absent in unfrustrated systems [8]. More unconventional behavior is displayed by the magnetization which is discontinuous in an external field as in the classical case, and the specific heat which has a two-peak structure as a function of temperature. For $s_i = 1$ non-magnetic excitations are still

present inside the singlet-triplet gap, and now there are two magnetization discontinuities in a field. Similar behavior with magnetization discontinuities was also found for the AHM on larger fullerene molecules of I_h symmetry for classical and $s_i = \frac{1}{2}$ spins [7]. There is strong evidence that this behavior is persistent for I_h symmetry in the $n \rightarrow \infty$ limit and survives asymptotically close to the zero and saturation fields, even though the number of hexagons strongly dominates the 12 frustrated pentagons.

Motivated by the non-trivial spectral and magnetic properties of the AHM on the I_h clusters, the $s_i = \frac{1}{2}$ AHM on fullerene clusters with symmetry other than I_h is investigated. Modine and Kaxiras calculated ground state energies and correlation functions of clusters with n up to 28, and by truncating the Hilbert space of a cluster with $n = 32$ [9]. They used no symmetries to reduce the computational requirements and found that same hexagon correlations are the most important for the minimization of the energy. For the $n = 28$ cluster more specifically the ground state was found to be doubly-degenerate. Their results are extended here with the calculation of the low-energy excitations and the response in a magnetic field for the clusters of Ref. [9] with $n = 24$ and 28, the most symmetric for these n values. The magnetic behavior of different clusters with $n = 26$ and 32 is investigated, as well as for a cluster with $n = 30$. All of them are shown in Fig. 1 [5, 10]. They are the most symmetric isomers for each n (for $n = 32$ the two clusters belong to different point groups who have the same number of symmetry operations). The spatial symmetry group along with the number of symmetry operations is listed in Table I for each n . The low energy spectra are calculated with Lanczos diagonalization, and point-group and spin-inversion symmetries are used to reduce the computational requirements and to classify the states according to the total symmetry group's irreducible representations [8]. Similarly to the I_h -symmetry

case it is of interest to look for non-magnetic states inside the singlet-triplet gap, and search for unconventional behavior of the magnetization and the possible presence of discontinuities in a field. Comparing with the case of the I_h clusters we gauge the effect of symmetry on the behavior of the AHM on the fullerenes. It is noted that fullerene clusters are edge- and not corner-sharing, and it is not obvious if it is possible to re-write the Hamiltonian as a sum of total spins on individual units or how to perform any other mathematical operations in order to derive analytic results, even in the classical limit.

From now on sites which belong only to pentagons will be called pentagon sites, while the rest will be called hexagon sites. The clusters will be abbreviated as C_n , with the D_{3d} $n = 32$ cluster $C_{32,I}$, and the D_{3h} $n = 32$ cluster $C_{32,II}$. Looking at Fig. 1, the pentagons form a band in the middle of C_{24} , while the hexagons a band in the middle of C_{30} and $C_{32,I}$. For C_{26} and C_{28} no hexagons are sharing edges, while for $C_{32,II}$ the hexagons are adjacent to each other in two groups of three. Close proximity of polygons of the same kind can in principle minimize frustration, which also decreases on the average with n . As seen in Table I and Fig. 2 the ground state energy per spin closely follows the aforementioned arguments. The clusters with $n = 30$ and 32 have the lowest energy per spin, as the hexagons approach each other more and more with increasing n . C_{24} has the next lowest energy with the band of pentagons separating the two hexagons. For C_{26} and C_{28} with the disconnected hexagons the energy is maximum, even higher than the dodecahedron (C_{20}) energy per spin, which is also plotted for comparison [8].

Frustration also results in non-magnetic excitations inside the singlet-triplet gap. The first excited state in all cases except C_{28} is a singly or doubly degenerate singlet (Tables II-VII, Fig. 3). For C_{30} and $C_{32,I}$ the second excited state is also a singlet, non-degenerate. In contrast, C_{28} 's first excited state is a triply degenerate triplet. For C_{24} , C_{30} and $C_{32,I}$ the low-lying singlets are well separated from the magnetic excitations. For all the clusters the dominant nearest-neighbor correlations in the ground states are of the intra-hexagon type, with intra-pentagon following closely (Table VIII). The only exception is $C_{32,II}$ where the intra-pentagon correlation is very strong and equal to -0.60548. This is appointed to the geometry of the cluster, with the "strong" bonds little frustrated in the middle of the structure and between the two groups of three hexagons each.

The magnetization in an external magnetic field does not present a discontinuity, as is the case for the dodecahedron [8]. There are only magnetization plateaux, where the ground state belongs to specific total spin S sectors for a wider range of fields than their neighboring sectors (Fig. 4). The most pronounced case is for $n = 28$ and $S = 2$. It appears that reducing the symmetry from I_h works against magnetization discontinuities.

The clusters considered in this paper have relatively small n and mostly belong to different spatial symmetry

groups. Only C_{26} and $C_{32,II}$ have the same spatial symmetry, nevertheless they have no common pattern of low energy and magnetic behavior as was the case for the I_h symmetry clusters [7, 8]. Similarities are only found in the low energy behavior of C_{30} and $C_{32,I}$ even though they belong to different symmetry groups, and they only have in common all the hexagons forming a band in the middle. It is also pointed out that there are some minor differences between the type I and type II molecules as they were called in Ref. [7], even though they both share the icosahedral I_h symmetry. Larger clusters can shed light on the magnetic properties as a function of the distribution of the pentagons, however this is not possible with present day computational means, at least for the low energy properties. Nevertheless, connectivity appears to be as important as spatial symmetry for the magnetic properties.

The plan of this paper is as follows: in section II the model and the method are introduced, and in section III the low energy spectra and nearest-neighbor correlation functions are presented. Section IV presents the results on the ground state magnetization, and section V the conclusions.

II. MODEL AND METHOD

The antiferromagnetic Heisenberg Hamiltonian with spins \vec{s}_i located on cluster vertices i is

$$H = J \sum_{\langle i,j \rangle} \vec{s}_i \cdot \vec{s}_j - hS^z \quad (1)$$

where $\langle \rangle$ denotes nearest neighbors, and J is positive and will be set equal to 1 from now on, defining the unit of energy. h is the strength of an external magnetic field and S^z the projection of the total spin along the field direction z . For an explanation of the use of symmetry operations to block-diagonalize the Hamiltonian, see Ref. [8] and references therein. The data for the symmetry groups was taken from Ref. [11]. Degeneracies are reported with respect to states with specific S , each of which corresponds to $2S + 1$ states with different value of S^z . Lanczos diagonalization was performed in double precision, but results are shown with a smaller number of significant digits to facilitate the presentation.

III. LOW ENERGY SPECTRA AND CORRELATION FUNCTIONS

The ground state energies per spin along with their degeneracies are listed in Table I. They are plotted as a function of n in Fig. 2. The bigger clusters achieve the lowest energy, while C_{26} and C_{28} the highest. Proximity of polygons of the same kind is crucial for energy minimization [9]. C_{26} and C_{28} do not have hexagons adjacent to each other (Fig. 1), and their energy per spin

is even higher than the corresponding energy for the dodecahedron, which has no hexagons [8]. They show that increase of the number of hexagons does not necessarily lead to lower energy per spin. For the bigger clusters the hexagons approach each other more and more and lower the energy, with $C_{32,II}$ having the lowest. Its structure is such that there are two groups of three adjacent hexagons each (Fig. 1(f)), and all hexagon-hexagon bond correlations are strong (Table VIII). In addition, there is a set of three pentagon-pentagon bonds in the middle of the cluster that have a very strong singlet character with a correlation value equal to -0.60548. Such a strong correlation is not achieved even within hexagons in any of the clusters, and points to the importance of the specific structure geometry rather than the symmetry for the minimization of the energy, at least for the fullerene clusters with small n considered in this paper. The two hexagon groups and the strong singlet-like pentagon bonds are correlated weakly with the rest of the spins.

The low energy spectra are shown in Tables II-VII and Fig. 3. Except from C_{28} , the ground and first excited states are singlets, with the ground states non-degenerate and the first excited states doubly degenerate except from C_{24} where it is non-degenerate. For C_{30} and $C_{32,I}$ the second excited state is also a singly degenerate singlet. As seen in Figs. 3(d) and 3(e) the low energy spectra of C_{30} and $C_{32,I}$ are similar. There is a non-degenerate singlet followed by two closely spaced singlets with the same degeneracy. The two clusters belong to different symmetry groups, but they both have their hexagons forming a band in the middle. Spin inversion symmetry is however opposite for the six lowest states in the spectra (Tables V and VI). C_{26} and $C_{32,II}$ on the other hand have the same spatial symmetry, D_{3h} . In their low energy spectra (Tables III and VII) the ground states belong to different irreducible representations, and their spin inversion symmetry is also different. The first excited states belong to the same irreducible representation, however the spin inversion symmetry is still different. This is in contrast to the smallest dodecahedral I_h symmetry clusters, the icosahedron (not of the fullerene type but made only of triangles) and the dodecahedron, which have similar structure and relative spacing of the levels in their low energy spectra even though they comprise of different polygons, therefore symmetry is a strong determining factor for their properties. This result points to the conclusion that spatial symmetry is not the only factor determining the low energy properties in general for the fullerenes.

C_{28} differs from the rest of the clusters in that its ground state is a doubly degenerate singlet [9], while the first excited state is a closely spaced triply degenerate triplet (Table IV). Then triply and doubly degenerate singlets follow, and the first non-degenerate state which has $S = 2$. In no other cluster an $S = 2$ state lies so low in the excitation spectrum. The ground state doublet belongs to the E_g representation, which transforms as the pair $(x^2 - y^2, 2z^2 - x^2 - y^2)$ of Cartesian tensors

[11]. In contrast to [9], here we find the correlations to be the same for both degenerate ground states. The ground state nearest neighbor correlation functions are shown in Table VIII for all the clusters. Except from the intra-pentagon correlation of $C_{32,II}$ same hexagon correlations are the strongest.

The nearest-neighbor correlation functions for the lowest singlet excitations are listed in table IX. The two smallest clusters and $C_{32,II}$ lower the energy of the hexagon-pentagon bonds while increasing the energy of the rest (only one of the same-hexagon bonds of C_{26} lowers very weakly). On the contrary, C_{30} behaves the other way, except from the intra-hexagon correlation in the middle of the cluster that refers to a common side of two hexagons, which weakens. Its two singlet excited states are very close in energy and in the behavior of the correlation functions, even though they are of different multiplicity, which is also true for $C_{32,I}$. The latter alters its same-hexagon bonds to generate the two excited singlets, even though the strongest one that refers to a common side of two hexagons does not change significantly.

The nearest-neighbor correlation functions for the first triplet excitation are shown in Table X. The values for $C_{32,II}$ change relatively little compared to the ground state, and the pentagon-pentagon correlation is getting even stronger. Similarly, C_{30} shows little change except from the hexagon-pentagon correlation that gets weaker. For C_{24} the triplet is mostly due to the decrease of the intra-hexagon correlation function, while in C_{26} the inter-hexagon correlation is getting stronger. In C_{28} only the inter-hexagon correlation $\langle \vec{S}_1 \cdot \vec{S}_5 \rangle$ changes relatively weakly compared to the other correlations, and correlation $\langle \vec{S}_{10} \cdot \vec{S}_{11} \rangle$ is particularly weak. Finally, for $C_{32,I}$ there are strong changes for all correlations except from $\langle \vec{S}_5 \cdot \vec{S}_{16} \rangle$.

IV. GROUND STATE MAGNETIZATION

The ground state magnetization as a function of an external field has typically a step-like structure, with a $\Delta S = 1$ discontinuity at fields where the ground state switches between adjacent S sectors. Frustration though can lead to magnetization discontinuities with $\Delta S > 1$, where a particular S sector never becomes the ground state in a field. Such is the case for the icosahedral symmetry I_h clusters, where the sector $S = \frac{n}{2} - 5$ with five flipped spins from saturation never includes the ground state [7]. The number of discontinuities is more than one at the classical level $S \rightarrow \infty$, and also for the dodecahedron ($n = 20$) and $s_i = 1$ where the calculation of the lowest energy state is computationally feasible for all S sectors (for I_h clusters with $n > 20$ the lowest energy state calculation is only possible for very high S even for $s_i = \frac{1}{2}$).

The lowest states for all the S sectors along with their degeneracies and the irreducible representation to which

they belong are listed in Table XI (the saturation fields are listed in Table I). The corresponding reduced magnetization $M = \frac{S}{ns_i}$ curves are shown in Fig. 4. Unlike the icosahedral symmetry case, no discontinuities are found.

For some values of M there are plateaux, where a particular S sector contains the ground state for a wider range of fields than the neighboring sectors. The most pronounced appears for C_{28} and $S = 2$, where $M = 0.14286$ (Fig. 4(c)).

It is again hard to draw correlations between symmetry and the response in a magnetic field. In Figs. 4(a) and 5(a) there is a correlation of the plateau-like features of the magnetization curve of C_{24} with stronger values of the intra-hexagon bonds. For C_{28} , where the singlet-triplet gap is very small, there are stronger intra-hexagon correlation functions for the few low-lying $S > 0$ sectors compared to the singlet case (Fig. 5(c)). There are S sectors that contain the ground state for a very narrow range of the field (Fig. 4(c)), and looking at Table XI their lowest state belongs to three-dimensional irreducible representations. For C_{30} , sectors $S = 3$ and 4 have very strong same-hexagon correlations, stronger than the ones in the ground state (Fig. 5(d)). For $C_{32,I}$ there are strong same-hexagon correlations for the low- S sectors, but for higher S intra-pentagon correlations are the strongest (Fig. 5(e)). In both cases, the strength of these correlations does not change significantly with the S value. $S = 12$ is the first sector that restores the same-hexagon correlations as the strongest, and it is the ground state for a narrow field window (Fig. 4(e)). In the case of $C_{32,II}$ there are low- S sectors where the intra-pentagon correlation is very strong (Fig. 5(f)). For $S = 1$ and 3 it is even stronger than the $S = 0$ value. For C_{26} the $S = 4$ and 6 sectors are ground states for a narrow range of the field (Fig. 4(b)) and same-hexagon correlations are weak (Fig. 5(b)). Finally, for C_{24} the single spin-flip subspace has the ground state for a very narrow window of the field (Fig. 4(a)), with the two spin-flip subspace having a plateau and the strongest intra-hexagon correlations relative to its neighboring S sectors (Fig. 5(a)).

For C_{26} and C_{28} the sector with a single spin flip from saturation is degenerate (Table XI). However, the spin flips are not confined on the hexagons except from the singly degenerate state of C_{26} , therefore there is no analogy with the high magnetization localized magnon states

discussed in Ref. [12].

V. CONCLUSIONS

The low energy spectrum and the magnetic response of the AHM have been calculated on a series of clusters with the connectivity of the fullerenes and a number of sites ranging from 24 to 32. Frustration and connectivity have a signature on the low energy spectrum with singlet ground and low energy excited states, the only exception being the 28-site cluster where the ground state is a doubly degenerate singlet and the first excited state a triplet. Frustration is minimal when pentagons and hexagons minimize their interference in the clusters by being placed adjacent to polygons of the same kind. The magnetization as a function of an external field exhibits plateau features, the most pronounced for $n = 28$ and $S = 2$. Unlike the icosahedral I_h symmetry clusters [7, 8], spatial symmetry is not the sole determining factor of the magnetic properties of the clusters and their connectivity appears to be important as well. It is desirable to investigate clusters of higher n to gain more insight on the correlation between symmetry, connectivity and magnetic properties, however this is very challenging with present day computational means, at least for the low energy properties. For low n the competition between unfrustrated hexagons and frustrated pentagons is strong, but even for high n the pentagon influence can be important, as in the case of I_h symmetry [7].

The author thanks D. Coffey for discussions. Most of the calculations were carried out at the Trinity Center for High Performance Computing at the University of Dublin. The work was supported by a Marie Curie Fellowship of the European Community program Development Host Fellowship under contract number HPMD-CT-2000-00048.

* Present address: Institut für Theoretische Physik A, Physikzentrum, RWTH Aachen, 52056 Aachen, Germany, Institut für Festkörperforschung-Theorie III, Forschungszentrum Jülich, Leo-Brandt-Strasse, 52425 Jülich, Germany and JARA-Fundamentals of Future Information Technology.

-
- [1] G. Misguich and C. Lhuillier, in *Frustrated Spin Systems*, edited by H.T. Diep (World Scientific, 2003).
 - [2] C. Lhuillier and P. Sindzingre, in *Quantum Properties of Low-Dimensional Antiferromagnets*, edited by Y. Ajiro and J. P. Boucher (Kyushu University Press, 2002).
 - [3] C. Lhuillier and G. Misguich, in *Lecture Notes in Physics (Springer Series) Vol. 595, "High Magnetic Fields Applications in Condensed Matter Physics and Spectroscopy"*, edited by C. Berthier, L. P. Levy and G. Martinez (Springer, 2001).
 - [4] J. Schnack, *Lect. Notes Phys.* **645**, 155 (2004).
 - [5] P. W. Fowler and D. E. Manolopoulos, *An Atlas of Fullerenes* (Oxford University Press, 1995).
 - [6] D. Coffey and S. A. Trugman, *Phys. Rev. Lett.* **69**, 176 (1992).
 - [7] N. P. Konstantinidis, *Phys. Rev. B* **76**, 104434 (2007).
 - [8] N. P. Konstantinidis, *Phys. Rev. B* **72**, 064453 (2005).
 - [9] N. A. Modine and E. Kaxiras, *Phys. Rev. B* **53**, 2546 (1996).
 - [10] M. Yoshida, <http://cochem2.tutkie.tut.ac.jp:8000/Fuller/>.

- [11] S. L. Altmann and P. Herzig, *Point-Group Theory Tables* (Oxford University Press, 1994).
 [12] J. Schulenburg, A. Honecker, J. Schnack, J. Richter, and H.-J. Schmidt, Phys. Rev. Lett. **88**, 167207 (2002).

TABLE I: Symmetry and ground state properties for the five clusters. $\frac{E_0}{n}$ is the ground state energy per spin and *mult.* is the state's multiplicity. h_{sat} is the saturation field.

sites n	symmetry group	number of symmetry operations	$\frac{E_0}{n}$	<i>mult.</i>	h_{sat}
24	D_{6d}	24	-0.48831	1	$4 + \sqrt{2}$
26	D_{3h}	12	-0.48496	1	$4 + \sqrt{2}$
28	T_d	24	-0.48482	2	$4 + \sqrt{2}$
30	D_{5h}	20	-0.49625	1	$3 + \sqrt{7}$
32 (I)	D_{3d}	12	-0.49597	1	$\frac{9+\sqrt{5}}{2}$
32 (II)	D_{3h}	12	-0.49804	1	5.61050

TABLE II: Low energy spectrum for C_{24} . E is the energy, *mult.* stands for the multiplicity of the state and *irrep.* for irreducible representation. S is the total spin, with each S state corresponding to $2S + 1$ states with different projection of the total spin along the z axis S^z . The spatial irreducible representation notation follows Ref. [11]. Indices s and a indicate the behavior under spin inversion, where s stands for symmetric and a for antisymmetric. A comma is introduced when necessary to avoid confusion between the notation for the spatial irreducible representation and the behavior under spin inversion.

E	<i>mult.</i>	<i>irrep.</i>	S	E	<i>mult.</i>	<i>irrep.</i>	S
-11.71937	1	$B_{1,s}$	0	-11.23652	2	$E_{2,a}$	1
-11.70478	1	$A_{1,s}$	0	-11.23043	1	$A_{1,s}$	0
-11.46814	2	$E_{3,a}$	1	-11.22852	2	$E_{1,a}$	1
-11.37244	1	$A_{2,a}$	1	-11.17883	2	$E_{3,a}$	1
-11.29779	1	$B_{1,s}$	0	-11.16437	2	$E_{4,s}$	0
-11.29326	2	$E_{2,s}$	0	-11.16257	2	$E_{1,s}$	0
-11.27888	1	$B_{2,a}$	1	-11.15826	2	$E_{3,s}$	0
-11.26341	2	$E_{5,a}$	1	-11.13896	2	$E_{4,a}$	1
-11.24565	2	$E_{5,s}$	0	-11.05126	1	$A_{1,s}$	0

TABLE III: Low energy spectrum for C_{26} . Notation as in table II.

E	<i>mult.</i>	<i>irrep.</i>	S	E	<i>mult.</i>	<i>irrep.</i>	S
-12.60898	1	$A'_{2,a}$	0	-12.31502	1	$A'_{2,a}$	0
-12.55739	2	E'_a	0	-12.30577	2	E'_s	1
-12.49297	2	E'_s	1	-12.28884	2	E'_s	1
-12.46174	1	$A''_{2,a}$	0	-12.26375	2	E''_a	0
-12.44862	1	$A''_{2,a}$	0	-12.21057	1	$A_{1,s}$	1
-12.42682	2	E'_a	0	-12.16192	2	E'_s	1
-12.42129	2	E'_s	1	-12.15183	2	$A_{1,a}$	0
-12.38217	1	$A'_{1,s}$	1	-12.14598	2	E'_s	1
-12.37889	1	$A'_{1,s}$	1	-12.13819	1	$A_{2,a}$	2

TABLE IV: Low energy spectrum for C_{28} . Notation as in table II.

E	<i>mult.</i>	<i>irrep.</i>	S	E	<i>mult.</i>	<i>irrep.</i>	S
-13.57486	2	E_s	0	-13.22866	3	$T_{2,a}$	1
-13.55978	3	$T_{2,a}$	1	-13.21762	1	$A_{1,s}$	0
-13.50468	3	$T_{2,s}$	0	-13.19914	3	$T_{2,s}$	0
-13.49099	2	E_s	0	-13.19486	3	$T_{1,a}$	1
-13.42327	1	$A_{1,s}$	2	-13.18471	2	E_s	0
-13.38652	2	E_a	1	-13.17446	3	$T_{2,a}$	1
-13.36105	3	$T_{2,a}$	1	-13.14963	1	$A_{2,s}$	0
-13.29319	3	$T_{1,s}$	0	-13.14309	1	$A_{1,a}$	1
-13.27818	3	$T_{1,a}$	1	-13.11265	3	$T_{2,s}$	2

TABLE V: Low energy spectrum for C_{30} . Notation as in table II.

E	<i>mult.</i>	<i>irrep.</i>	S	E	<i>mult.</i>	<i>irrep.</i>	S
-14.88742	1	$A''_{2,a}$	0	-14.47476	1	$A''_{2,a}$	0
-14.83815	2	$E''_{2,a}$	0	-14.46287	2	$E''_{2,s}$	1
-14.82517	1	$A'_{2,a}$	0	-14.45130	2	$E'_{1,s}$	1
-14.62495	1	$A_{1,s}$	1	-14.33694	2	$E'_{1,a}$	0
-14.60458	2	$E_{2,s}$	1	-14.27711	2	$E'_{1,a}$	0
-14.59928	1	$A'_{1,s}$	1	-14.26727	1	$A'_{2,a}$	0
-14.51907	2	$E'_{1,s}$	1	-14.23932	1	$A'_{1,s}$	1
-14.50190	2	$E''_{1,a}$	0	-14.17268	2	$E''_{2,s}$	1
-14.48316	2	$E'_{2,s}$	1	-14.16221	1	$A_{2,a}$	2

TABLE VI: Low energy spectrum for $C_{32,I}$. Notation as in table II.

E	mult.	irrep.	S	E	mult.	irrep.	S
-15.87092	1	$A_{1u,s}$	0	-15.49168	1	$A_{2g,a}$	1
-15.81199	2	$E_{g,s}$	0	-15.47080	1	$A_{1u,s}$	0
-15.80648	1	$A_{1g,s}$	0	-15.46339	1	$A_{1u,a}$	1
-15.67299	2	$E_{u,a}$	1	-15.45531	2	$E_{g,a}$	1
-15.59634	2	$E_{g,a}$	1	-15.44665	2	$E_{u,s}$	0
-15.57987	1	$A_{2u,a}$	1	-15.44513	2	$E_{g,a}$	1
-15.52875	2	$E_{g,s}$	0	-15.43356	1	$A_{2g,a}$	1
-15.51890	1	$A_{1g,s}$	0	-15.38287	1	$A_{1g,s}$	2
-15.49978	2	$E_{u,a}$	1	-15.38034	1	$A_{2u,a}$	1

TABLE VII: Low energy spectrum for $C_{32,II}$. Notation as in table II.

E	mult.	irrep.	S	E	mult.	irrep.	S
-15.93723	1	$A_{1,s}''$	0	-15.50045	1	$A_{2,a}''$	1
-15.81192	2	E_s'	0	-15.49288	1	$A_{1,s}''$	0
-15.77366	1	$A_{2,a}'$	1	-15.46219	1	$A_{1,s}'$	0
-15.73368	1	$A_{1,s}'$	0	-15.45437	1	$A_{2,a}'$	1
-15.63730	2	E_a'	1	-15.45317	1	$A_{1,a}'$	1
-15.60167	2	E_a'	1	-15.42185	2	E_s''	0
-15.57485	2	E_s''	0	-15.39363	1	$A_{2,a}''$	1
-15.56589	2	E_a''	1	-15.38231	1	$A_{2,a}''$	1
-15.54070	2	E_a''	1	-15.38020	2	E_a''	1

TABLE VIII: Distinct nearest-neighbor correlation functions for the ground states.

sites n	intra-hexagon	inter-hexagon	hexagon-pentagon	intra-pentagon
24	$\langle \vec{S}_1 \cdot \vec{S}_2 \rangle = -0.40325$		$\langle \vec{S}_1 \cdot \vec{S}_7 \rangle = -0.20285$	$\langle \vec{S}_7 \cdot \vec{S}_8 \rangle = -0.37051$
26	$\langle \vec{S}_5 \cdot \vec{S}_7 \rangle = -0.33858$ $\langle \vec{S}_5 \cdot \vec{S}_{11} \rangle = -0.42436$	$\langle \vec{S}_{11} \cdot \vec{S}_{12} \rangle = -0.10317$	$\langle \vec{S}_2 \cdot \vec{S}_5 \rangle = -0.26523$	$\langle \vec{S}_1 \cdot \vec{S}_2 \rangle = -0.33215$
28	$\langle \vec{S}_1 \cdot \vec{S}_2 \rangle = -0.35418$	$\langle \vec{S}_1 \cdot \vec{S}_5 \rangle = -0.23883$	$\langle \vec{S}_2 \cdot \vec{S}_3 \rangle = -0.30347$	
30	$\langle \vec{S}_6 \cdot \vec{S}_7 \rangle = -0.36221$ $\langle \vec{S}_7 \cdot \vec{S}_{18} \rangle = -0.35466$		$\langle \vec{S}_1 \cdot \vec{S}_6 \rangle = -0.24081$	$\langle \vec{S}_1 \cdot \vec{S}_2 \rangle = -0.34618$
32 (D_{3d})	$\langle \vec{S}_5 \cdot \vec{S}_6 \rangle = -0.37205$ $\langle \vec{S}_5 \cdot \vec{S}_{16} \rangle = -0.32629$ $\langle \vec{S}_{11} \cdot \vec{S}_{12} \rangle = -0.24979$ $\langle \vec{S}_{11} \cdot \vec{S}_{19} \rangle = -0.45409$		$\langle \vec{S}_2 \cdot \vec{S}_6 \rangle = -0.30381$	$\langle \vec{S}_1 \cdot \vec{S}_2 \rangle = -0.30903$
32 (D_{3h})	$\langle \vec{S}_1 \cdot \vec{S}_2 \rangle = -0.36273$ $\langle \vec{S}_2 \cdot \vec{S}_5 \rangle = -0.35602$ $\langle \vec{S}_5 \cdot \vec{S}_{11} \rangle = -0.41480$	$\langle \vec{S}_{11} \cdot \vec{S}_{22} \rangle = -0.24352$	$\langle \vec{S}_5 \cdot \vec{S}_{14} \rangle = -0.16367$	$\langle \vec{S}_{14} \cdot \vec{S}_{15} \rangle = -0.60548$

TABLE IX: Distinct nearest-neighbor correlation functions for the singlet excited states within the singlet-triplet gap.

sites n	intra-hexagon	inter-hexagon	hexagon-pentagon	intra-pentagon
24	$\langle \vec{S}_1 \cdot \vec{S}_2 \rangle = -0.37785$		$\langle \vec{S}_1 \cdot \vec{S}_7 \rangle = -0.25586$	$\langle \vec{S}_7 \cdot \vec{S}_8 \rangle = -0.34169$
26	$\langle \vec{S}_5 \cdot \vec{S}_7 \rangle = -0.28615$ $\langle \vec{S}_5 \cdot \vec{S}_{11} \rangle = -0.42640$	$\langle \vec{S}_{11} \cdot \vec{S}_{12} \rangle = -0.084111$	$\langle \vec{S}_2 \cdot \vec{S}_5 \rangle = -0.30251$	$\langle \vec{S}_1 \cdot \vec{S}_2 \rangle = -0.30687$
30	$\langle \vec{S}_6 \cdot \vec{S}_7 \rangle = -0.37609$ $\langle \vec{S}_7 \cdot \vec{S}_{18} \rangle = -0.33026$		$\langle \vec{S}_1 \cdot \vec{S}_6 \rangle = -0.21102$	$\langle \vec{S}_1 \cdot \vec{S}_2 \rangle = -0.35548$
30	$\langle \vec{S}_6 \cdot \vec{S}_7 \rangle = -0.37784$ $\langle \vec{S}_7 \cdot \vec{S}_{18} \rangle = -0.32507$		$\langle \vec{S}_1 \cdot \vec{S}_6 \rangle = -0.20832$	$\langle \vec{S}_1 \cdot \vec{S}_2 \rangle = -0.35598$
32 (D_{3d})	$\langle \vec{S}_5 \cdot \vec{S}_6 \rangle = -0.39744$ $\langle \vec{S}_5 \cdot \vec{S}_{16} \rangle = -0.29843$ $\langle \vec{S}_{11} \cdot \vec{S}_{12} \rangle = -0.27220$ $\langle \vec{S}_{11} \cdot \vec{S}_{19} \rangle = -0.45947$		$\langle \vec{S}_2 \cdot \vec{S}_6 \rangle = -0.30566$	$\langle \vec{S}_1 \cdot \vec{S}_2 \rangle = -0.29805$
32 (D_{3d})	$\langle \vec{S}_5 \cdot \vec{S}_6 \rangle = -0.40407$ $\langle \vec{S}_5 \cdot \vec{S}_{16} \rangle = -0.30669$ $\langle \vec{S}_{11} \cdot \vec{S}_{12} \rangle = -0.27231$ $\langle \vec{S}_{11} \cdot \vec{S}_{19} \rangle = -0.45357$		$\langle \vec{S}_2 \cdot \vec{S}_6 \rangle = -0.29314$	$\langle \vec{S}_1 \cdot \vec{S}_2 \rangle = -0.30482$
32 (D_{3h})	$\langle \vec{S}_1 \cdot \vec{S}_2 \rangle = -0.36028$ $\langle \vec{S}_2 \cdot \vec{S}_5 \rangle = -0.34068$ $\langle \vec{S}_5 \cdot \vec{S}_{11} \rangle = -0.41156$	$\langle \vec{S}_{11} \cdot \vec{S}_{22} \rangle = -0.16865$	$\langle \vec{S}_5 \cdot \vec{S}_{14} \rangle = -0.24184$	$\langle \vec{S}_{14} \cdot \vec{S}_{15} \rangle = -0.40508$

TABLE X: Distinct nearest-neighbor correlation functions for the first triplet excited states.

sites n	intra-hexagon	inter-hexagon	hexagon-pentagon	intra-pentagon
24	$\langle \vec{S}_1 \cdot \vec{S}_2 \rangle = -0.38523$		$\langle \vec{S}_1 \cdot \vec{S}_7 \rangle = -0.20358$	$\langle \vec{S}_7 \cdot \vec{S}_8 \rangle = -0.36686$
26	$\langle \vec{S}_5 \cdot \vec{S}_7 \rangle = -0.34294$ $\langle \vec{S}_5 \cdot \vec{S}_{11} \rangle = -0.40945$	$\langle \vec{S}_{11} \cdot \vec{S}_{12} \rangle = -0.13733$	$\langle \vec{S}_2 \cdot \vec{S}_5 \rangle = -0.25900$	$\langle \vec{S}_1 \cdot \vec{S}_2 \rangle = -0.33365$
28	$\langle \vec{S}_1 \cdot \vec{S}_2 \rangle = -0.32073$ $\langle \vec{S}_4 \cdot \vec{S}_5 \rangle = -0.42032$ $\langle \vec{S}_2 \cdot \vec{S}_{10} \rangle = -0.42541$	$\langle \vec{S}_1 \cdot \vec{S}_5 \rangle = -0.22540$ $\langle \vec{S}_{10} \cdot \vec{S}_{11} \rangle = -0.010665$	$\langle \vec{S}_2 \cdot \vec{S}_3 \rangle = -0.33309$ $\langle \vec{S}_3 \cdot \vec{S}_4 \rangle = -0.16012$	
30	$\langle \vec{S}_6 \cdot \vec{S}_7 \rangle = -0.35985$ $\langle \vec{S}_7 \cdot \vec{S}_{18} \rangle = -0.34801$		$\langle \vec{S}_1 \cdot \vec{S}_6 \rangle = -0.22022$	$\langle \vec{S}_1 \cdot \vec{S}_2 \rangle = -0.34857$
32 (D_{3d})	$\langle \vec{S}_5 \cdot \vec{S}_6 \rangle = -0.40953$ $\langle \vec{S}_5 \cdot \vec{S}_{16} \rangle = -0.33089$ $\langle \vec{S}_{11} \cdot \vec{S}_{12} \rangle = -0.28203$ $\langle \vec{S}_{11} \cdot \vec{S}_{19} \rangle = -0.42064$		$\langle \vec{S}_2 \cdot \vec{S}_6 \rangle = -0.25415$	$\langle \vec{S}_1 \cdot \vec{S}_2 \rangle = -0.32989$
32 (D_{3h})	$\langle \vec{S}_1 \cdot \vec{S}_2 \rangle = -0.35863$ $\langle \vec{S}_2 \cdot \vec{S}_5 \rangle = -0.35762$ $\langle \vec{S}_5 \cdot \vec{S}_{11} \rangle = -0.40890$	$\langle \vec{S}_{11} \cdot \vec{S}_{22} \rangle = -0.24266$	$\langle \vec{S}_5 \cdot \vec{S}_{14} \rangle = -0.15494$	$\langle \vec{S}_{14} \cdot \vec{S}_{15} \rangle = -0.61209$

TABLE XI: Lowest energies (E_0), multiplicities ($mult.$) and corresponding irreducible representations ($irrep.$) in each total spin S sector for the clusters. The spatial irreducible representation notation follows Ref. [11]. Indices s and a indicate the behavior under spin inversion, where s stands for symmetric and a for antisymmetric. It is only possible to calculate them for states lying relatively low or high in the energy spectrum. A comma is introduced when necessary to avoid confusion between the notation for the spatial irreducible representation and the behavior under spin inversion.

	C_{24}	C_{24}	C_{24}	C_{26}	C_{26}	C_{26}	C_{28}	C_{28}	C_{28}
S	E_0	$mult.$	$irrep.$	E_0	$mult.$	$irrep.$	E_0	$mult.$	$irrep.$
0	-11.71937	1	$B_{1,s}$	-12.60898	1	$A'_{2,a}$	-13.57486	2	E_s
1	-11.46814	2	$E_{3,a}$	-12.49297	2	E'_s	-13.55978	3	$T_{2,a}$
2	-10.92259	1	$B_{1,s}$	-12.13819	1	$A'_{2,a}$	-13.42327	1	$A_{1,s}$
3	-10.13390	1	$B_{2,a}$	-11.39120	1	$A'_{1,s}$	-12.45085	3	$T_{2,a}$
4	-8.88178	1	$A_{1,s}$	-10.16420	1	$A'_{2,a}$	-11.45102	1	$A_{1,s}$
5	-7.28948	2	E_5	-8.83042	1	$A'_{1,s}$	-10.18889	1	$A_{1,a}$
6	-5.49575	1	A_1	-7.01596	1	A'_2	-8.51700	1	A_1
7	-3.46016	1	B_2	-5.07125	1	A'_1	-6.56848	3	T_2
8	-1.24214	1	B_1	-2.91337	2	E'	-4.52626	2	E
9	1.10955	1	A_2	-0.62134	2	E'	-2.32108	1	A_1
10	3.59067	1	$B_{1,s}$	1.75066	1	A'_2	-0.049533	1	A_1
11	6.29289	2	$E_{3,a}$	4.36198	1	A'_1	2.48354	3	T_2
12	9	1	$A_{1,s}$	7.04289	1,2	$A'_{2,a}, E'$	5.11292	2	E
13				9.75	1	$A'_{1,s}$	7.79289	1,3	$A_{1,a}, T_2$
14							10.5	1	$A_{1,s}$
	C_{30}	C_{30}	C_{30}	$C_{32,I}$	$C_{32,I}$	$C_{32,I}$	$C_{32,II}$	$C_{32,II}$	$C_{32,II}$
S	E_0	$mult.$	$irrep.$	E_0	$mult.$	$irrep.$	E_0	$mult.$	$irrep.$
0	-14.88742	1	$A''_{2,a}$	-15.87092	1	$A_{1u,s}$	-15.93723	1	$A''_{1,s}$
1	-14.62495	1	$A'_{1,s}$	-15.67299	2	$E_{u,a}$	-15.77366	1	$A'_{2,a}$
2	-14.16221	1	$A'_{2,a}$	-15.38287	1	$A_{1g,s}$	-15.35876	1	A_1
3	-13.47738	2	$E'_{2,s}$	-14.72334	1	A_{2g}	-14.68665	1	A'_2
4	-12.52542	1	A''_2	-13.83231	1	A_{1g}	-13.80765	1	A'_1
5	-11.26275	1	A''_1	-12.66407	1	A_{2g}	-12.59064	1	A'_1
6	-9.71967	2	E''_2	-11.25111	1	A_{1g}	-11.12132	1	A''_1
7	-7.94218	2	E'_2	-9.56173	1	A_{2g}	-9.42233	1	A'_1
8	-6.07738	1	A''_2	-7.65604	1	A_{1g}	-7.61188	1	A'_1
9	-3.98134	1	A''_1	-5.59828	1	A_{2g}	-5.58108	1	A''_2
10	-1.69706	1	A'_2	-3.40688	1	A_{1g}	-3.43626	1	A'_1
11	0.66164	1	A'_1	-1.06488	1	A_{2g}	-1.14953	1	A''_2
12	3.08988	1	A''_2	1.37454	1	A_{2g}	1.25805	1	A'_1
13	5.68792	1	A'_1	3.84610	1	A_{2g}	3.79378	1	A''_2
14	8.42712	1	A''_2	6.44732	1	A_{1g}	6.42049	1	A'_1
15	11.25	1	$A'_{1,s}$	9.19098	1	A_{2g}	9.19475	1	A''_2
16				12	1	$A_{1g,s}$	12	1	$A'_{1,s}$

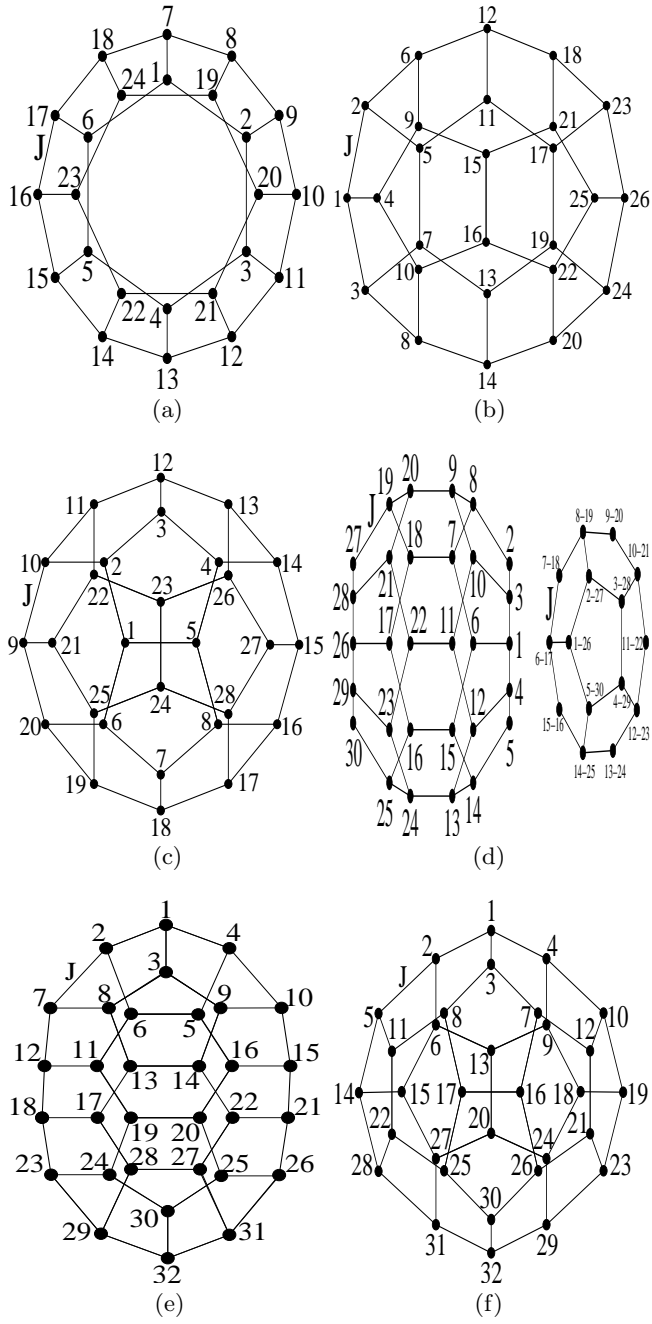


FIG. 1: Projection of the clusters on a plane: (a) C_{24} , (b) C_{26} , (c) C_{28} , (d) C_{30} (e) $C_{32,I}$ and (f) $C_{32,II}$. For C_{30} there is also a top (bottom with the dashes) view. The black circles are spins s_i . The solid lines are antiferromagnetic bonds J .

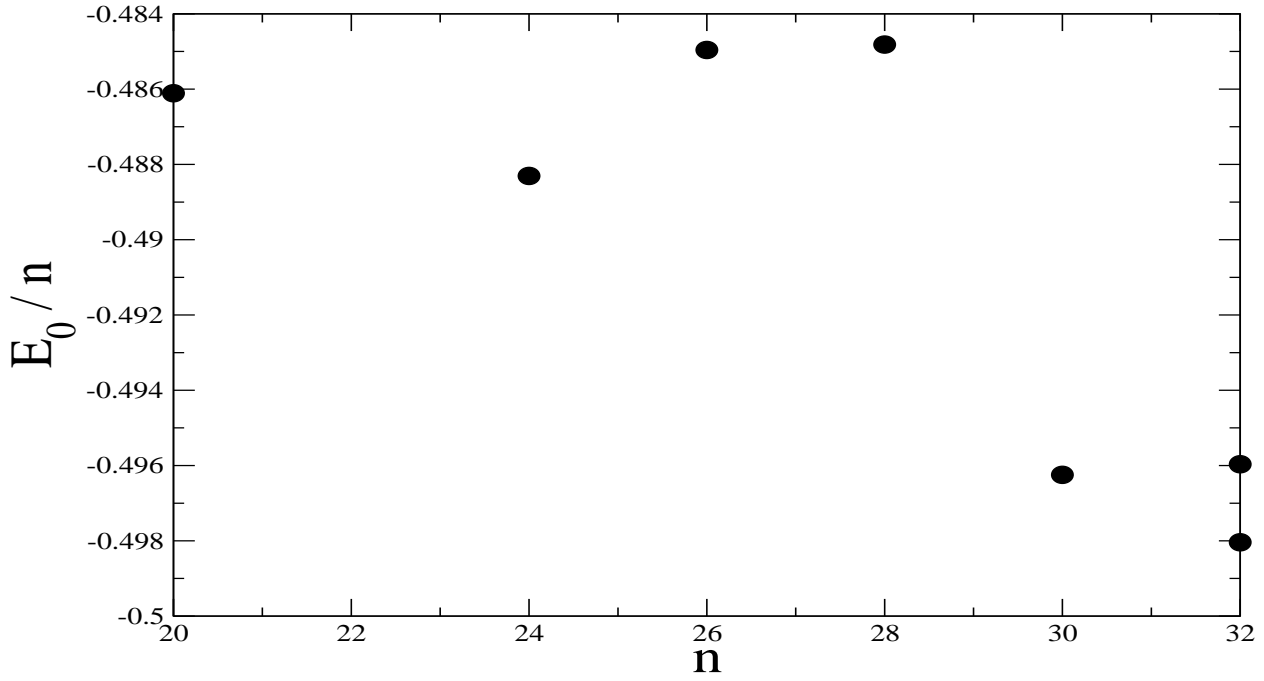


FIG. 2: Ground state energy per spin $\frac{E_0}{n}$ as a function of the number of spins n . The value for $n = 20$ is taken from [8]. The lowest energy for $n = 32$ is for cluster $C_{32,II}$, and the highest for $C_{32,I}$.

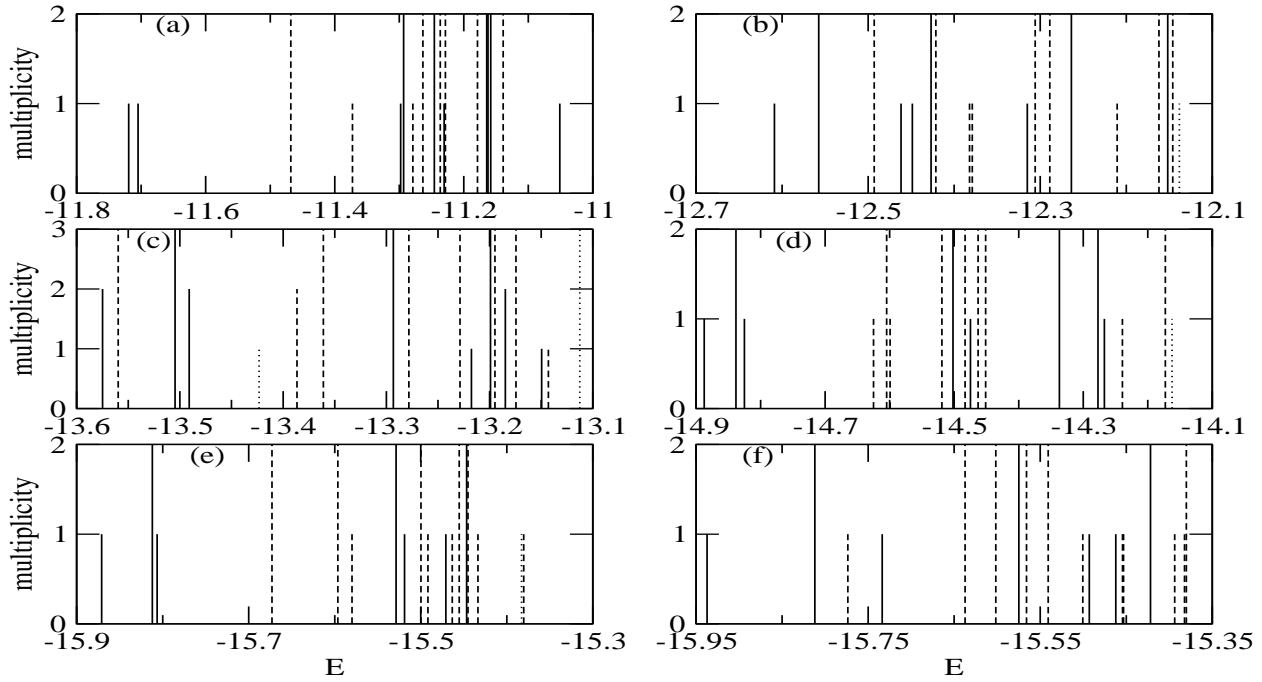


FIG. 3: Low energy E spectrum of total spin S states and its multiplicity: (a) C_{24} , (b) C_{26} , (c) C_{28} , (d) C_{30} (e) $C_{32,I}$ and (f) $C_{32,II}$. Solid lines: $S = 0$, dashed lines: $S = 1$, dotted lines: $S = 2$.

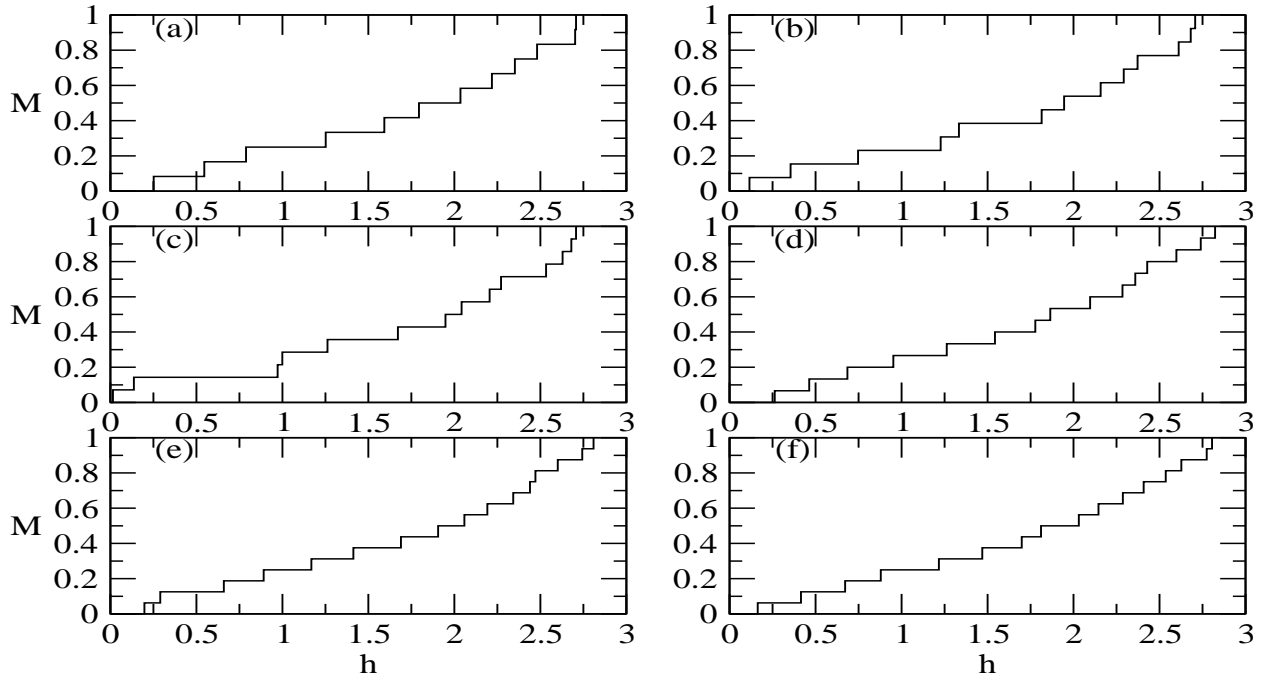


FIG. 4: Reduced ground state magnetization $M = \frac{S}{ns_i}$ as a function of magnetic field h : (a) C_{24} , (b) C_{26} , (c) C_{28} , (d) C_{30} , (e) $C_{32,I}$ and (f) $C_{32,II}$. M is the total spin S normalized to the number of sites n and the magnitude of spin s_i . M has no units and h is in units of energy.

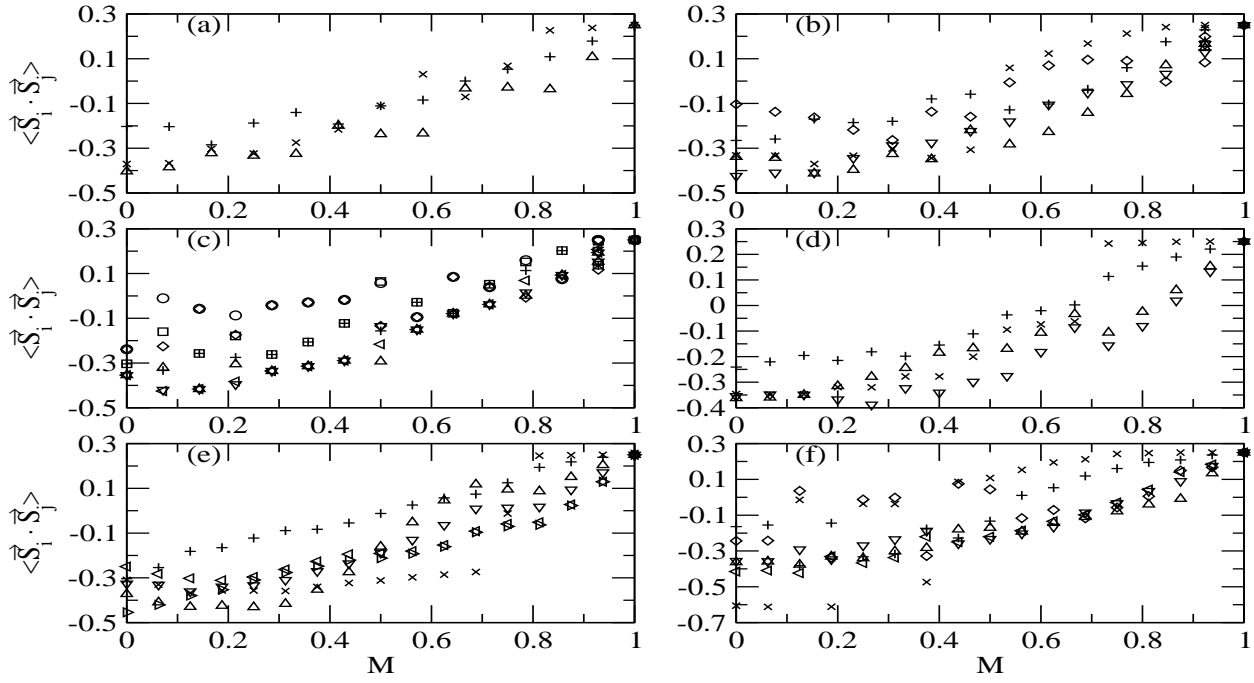


FIG. 5: Distinct correlation functions for the lowest energy state in each total spin S sector: (a) C_{24} , (b) C_{26} , (c) C_{28} , (d) C_{30} , (e) $C_{32,I}$ and (f) $C_{32,II}$. The reduced magnetization $M = \frac{S}{ns_i}$ is the total spin S normalized to the number of sites n and the magnitude of spin s_i . $\langle \vec{S}_i \cdot \vec{S}_j \rangle$ is in units of energy and M has no units. $\langle \vec{S}_i \cdot \vec{S}_j \rangle$: \triangle , \triangleleft , \triangleright , ∇ : intra-hexagon, \diamond , \circ : inter-hexagon, $+$, \square : hexagon-pentagon, \times : intra-pentagon.